Published in: Chemical Physics (1996), vol. 206, pp. 225-236.
Status: Postprint (Author's version)

The appearance of CH_3^+ ions from methyl halides by non-resonant photoionization. A translational energy surprisal analysis. Part I. CH_3F

J. Momigny, R. Locht

Département de Chimie Générale et de Chimie Physique, Institut de Chimie, Bat. B6c, Université de Liège, Sart-Tilman, B-4000 Liège 1, Belgium

Abstract

A surprisal analysis has been applied to the total translational energy distribution (TED) of $CH_3^+ + F$ from CH_3F giving rise to a new and deeper insight into the dissociation dynamics involved in this process. For both the 16.85 and 21.22 eV photon energies used, the direct population at different energy levels of the B ^2E state of CH_3F^+, which is radiationlessly coupled to the repulsive CH_3F^+ (A^2A_1) state, gives rise to wide and negatively surprised total TEDs. At both energies they have to be ascribed to severe limitations in the vibrational excitation of CH_3^+. Additionally, in the case of 21.22 eV photons, a non-statistical expression has to be used to account for the density of translational states. At both photon energies, the population of the CH_3F^+ electronic states through autoionization of Rydberg states accounts for (i) the concurrent appearance of TEDs governed by a pure RRKM behaviour and (ii) the positively surprised TEDs where the angular momentum conservation plays an important role. At 16.85 eV photon energy the distributions are assigned to $CH_3F^+(X\ ^2E) \rightarrow CH_3\ (X\ ^1A'_1) + F$. At 21.22 eV photon energy, doubly excited electronic states of CH_3F^+ are assumed to take part and they are correlated with CH_3^+ ($^3A''$) + F channel.

1. Introduction

It has been recently shown how the occurrence of a bimodal behaviour in the translational energy surprisal of the $C_2H_3^+$+F dissociation products from C_2H_3F could be assigned to the existence of two mechanisms in the dynamics of the dissociation process [1]. This experience led us to reinvestigate the surprisal of the translational energy distribution (TED) associated with the $CH_3^+ + X$ (X = F, Cl, Br, I) decomposition from the methylhalides. A critical review of the large number of contributions devoted to different aspects of the ionization phenomena in these molecules, together with the present results, will enlighten the processes where the same ion (CH_3^+) appears from one class of precursors. The large amount of information obtained from the present investigation accounts for this contribution. The same CH_3^+ producing process observed in CH_3X (X = Cl, Br, I) will be reported in a forthcoming paper.

2. Experimental results

The translational energy distribution of CH_3^+ from CH_3F is measured by using the experimental setup already described previously [2].

Briefly the photoions are formed in a Nier-type ion source with the VUV light produced in a discharge in rare gases, i.e. He (58.4 nm/21.22 eV) and Ne (73.6-74.4 nm/16.85-16.67 eV). Between the focusing lens and the entrance hole of a quadrupole mass spectrometer, the ions are energy analyzed by a retarding lens.

The observed TEDs of CH_3^+ obtained with the Ne(I) and the He(I) resonance lines are represented in Fig. 1a. Using the momentum conservation law, these distributions have been converted in terms of total TEDs corresponding to the energy carried away by the dissociation products $CH_3^+ + F$. The result of this conversion is shown in Fig. lb.

3. Evaluation of the translational energy surprisal

In a first contribution on this subject [3] the translational energy surprisals have been erroneously calculated for a unique value of the excess energy *E* corresponding to the difference (*hv* — AE) where *hv* is the photon energy and AE is the calculated appearance energy of CH_3^+. As pointed out later [1], in an ideal experiment a total TED would be measured simultaneously with successively increased values of the energy *E* in excess with respect to the lowest dissociation limit. In the present experiment the measured total TED is the result of the sum of such distributions, each being weighted for the ionic abundance observed for each energy value *E* under the same experimental conditions. Therefore it follows that any a priori calculated TED suitable for a surprisal evaluation will also be a similarly weighted sum of a priori calculated total TED for successively selected values of the excess energy *E*.

Published in: Chemical Physics (1996), vol. 206, pp. 225-236.
Status: Postprint (Author's version)

Fig. 1. *(a) Experimental translational energy distributions and (b) total TED deduced from (a) for the process $CH_3F^+ \rightarrow CH_3^+ + F$ and obtained with the Ne(I) resonance lines or 16.85 eV photons (Ne) and with the He(I) resonance line or 21.22 eV photons (He).*

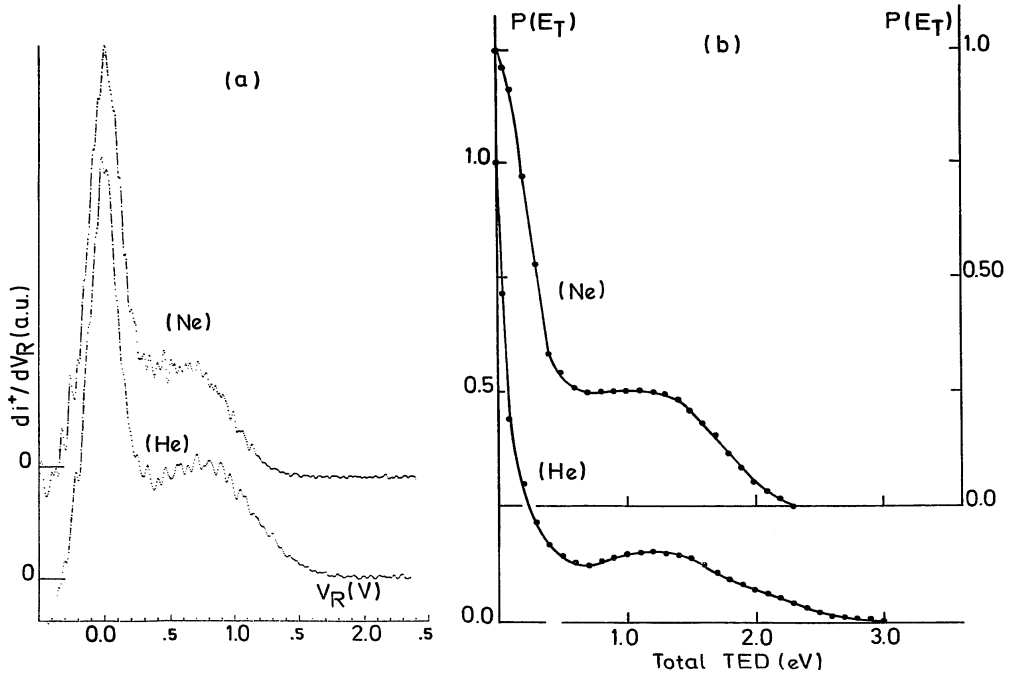

Fig. 2*. The appearance of CH_3^+ from CH_3F. (a) Idealized He(I) photoelectron spectrum of CH_3F, (b) excitation energies E for $CH_3^+ + F$ with 16.85 eV photons (Nefl)) and 21.22 eV photons (He(I)) and (c) energy interval available for $CH_3^+ + F$ production through direct ionization.*

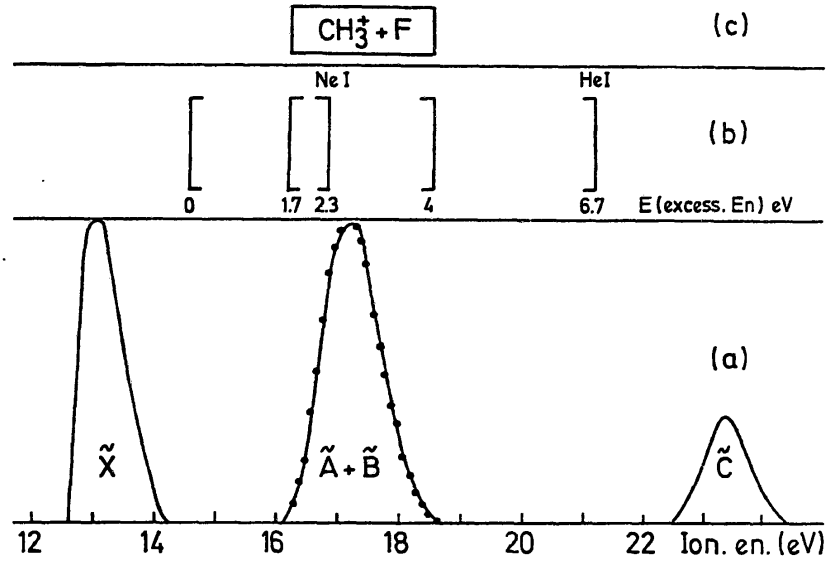

From Fig. 2, and taking 14.55 eV as the calculated and experimental threshold energy for the production of CH_3^+ ions [4], for 16.85 eV photons the excess energy E ranges from 0.0 to 2.3 eV and for 21.22 eV photon energy the excess energy E varies from 0.0 to 6.7 eV.

However, as shown by photoion-photoelectron coincidence (PIPECO) experiments [5] the appearance of CH_3^+ by the direct dissociative ionization channel is only opened through the CH_3F^+ ($A^2A_1 + B\ ^2E$) states. From the photoelectron spectrum of CH_3F represented in Fig. 2 [6,7] the excess energy range of E will be restricted to the interval of 1.7 eV $\leq E \leq$ 2.3 eV and 1.7 eV $\leq E \leq$ 4.0 eV for the Ne(I) and He(I) resonance lines respectively.

Published in: Chemical Physics (1996), vol. 206, pp. 225-236.
Status: Postprint (Author's version)

Fig. 3. *Surprisal plots for the total TED as obtained by (a) 16.85 eV photons and (b) 21.22 eV photons. They exhibit a linear surprisal for 0.075 eV ≤ E_T ≤ 0.4 eV in the former and for 0.7 eV < E_T ≤ 2.3 eV in the latter.*

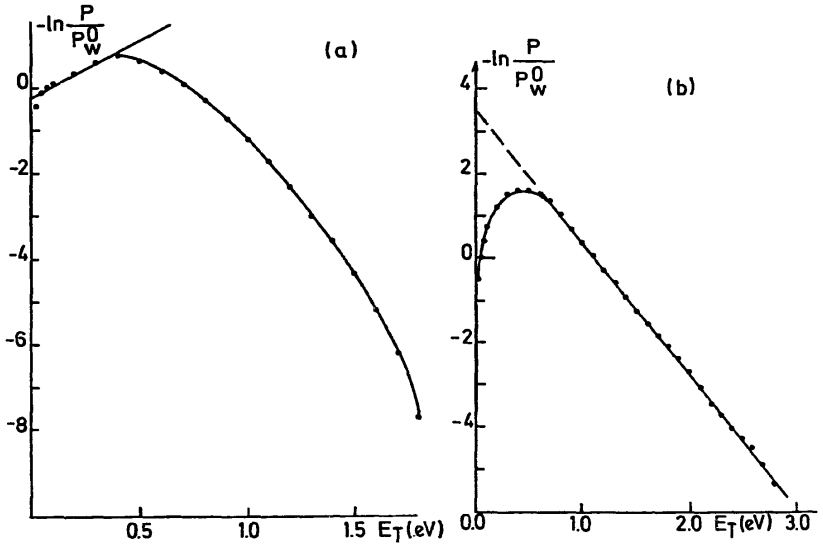

In order to calculate the a priori weighted statistical total TED, i.e. P_w^0 expressed by

$$P_w^0 = \sum_i a_i P^0(E_T/E_i), \qquad (1)$$

used for the surprisal evaluation of the distributions represented in Fig. lb, the $P^0(E_T/E_i)$ distributions have been calculated for E_i values included in the ranges of 1.7 eV ≤ E_i ≤ 2.3 eV and 1.7 eV ≤ E_i ≤ 4.0 eV by steps of 0.1 eV using the RRHO approximation [1] i.e.

$$P_0(E_T/E_i) = C_i E_T^{0.5}(E_i - E_T)^{s+r/2-1}, \qquad (2)$$

where s and r represent the number of vibrational and rotational degrees of freedom of CH_3^+ respectively and C_i stands for a constant disappearing by a an appropriate normalization to the maximum of the calculated distribution. In the case of CH_3^+ s = 6 and r = 3 and Eq. (1) becomes

$$P_w^0 = \sum_i a_i E_T^{0.5}(E_i - E_T)^{6.5}. \qquad (3)$$

The weighting factors a_i are measured for each step i from the photoelectron band corresponding to the (A^2A_1 +B ^{2}E) states and drawn in Fig. 2. Keeping in mind that the surprisal P is expressed by

$$P = -\ln P(E_T)/P_w^0, \qquad (4)$$

the calculations mentioned above give rise to the surprisal diagrams represented in Fig. 3 for Ne(I) (see Fig. 3a) and He(I) (see Fig. 3b) excitation respectively. These diagrams will be discussed separately below.

3.1. The surprisal observed with the Ne(I) lines

The surprisal plot 3a has a complex shape. It reaches a maximum at 0.4 eV translational energy, is mainly linear for 0.05 eV ≤ E_T≤ 0.4 eV and exhibits a strong curvature for 0.5 eV ≤ E_T ≤ 2.2 eV. By a least-squares fit the linear portion of the surprisal is expressed by

$$-\ln P(E_T)/P_w^0 = -0.15 + 2.24E_T. \qquad (5)$$

From this equation the values of P(E_T) corresponding to Eq. (3) have been calculated and subtracted from the

Published in: Chemical Physics (1996), vol. 206, pp. 225-236.
Status: Postprint (Author's version)

experimental distribution in Fig. lb (Ne). The results of this treatment in shown in Fig. 4a. The total TED appears as resulting from the superposition of three distributions: (i) a zero translational energy distribution P_0, (ii) a TED of the form given by Eq. (2) for 0.0 eV $\leq E_T \leq$ 1.2 eV and designated by P_1, and (iii) a P_2 distribution for the total translational energy range 0.4 eV $\leq E_T \leq$ 2.3 eV.

3.2. The surprisal observed with the He(I) line

The surprisal plot of Fig. 3b is related to the total TED observed with the He(I) line (see Fig. lb (He)). This distribution shows a long linear behaviour in the range 0.7 eV $\leq E_T \leq$ 3.0 eV represented by the least-squares fit

$$-\ln P(E_T)/P_w^0 = 3.48 - 3.133\,E_T \qquad (6)$$

Introducing the relationship (3) for P_w^0 in Eq. (6) the whole distribution has been calculated down to E_T = 0.0 eV and is subtracted from the experimental data (see Fig. lb (He)). The result is represented in Fig. 4b and differs appreciably from the result obtained with the Ne(I) resonance lines. The experimental distribution should be a sum of two contributions starting both at E_T = 0.0 eV: (i) a rather narrow distribution in the range 0.0 eV $\leq E_T \leq$ 0.7 eV with a maximum centred on E_T = 0.0 eV and designated by P_1, (ii) a wide total TED designated by P_2 starting at E_T = 0.0 eV where $P(E_T)$ = 0 and extending over the range 0.0 eV $\leq E_T \leq$ 3.0 eV.

Both these complex and differing situations observed for Ne(I) and He(I) will be discussed in detail in the following section.

Fig. 4 *Deconvolution of the total TED as obtained with (a) 16.85 eV photons and (b) 21.22 eV photons and calculated from the data of Fig. 3a and Fig. 3b respectively. The former is decomposed into three distributions P_0, P_1 and P_2. The latter is found to be the sum of two distributions P_1 and P_2.*

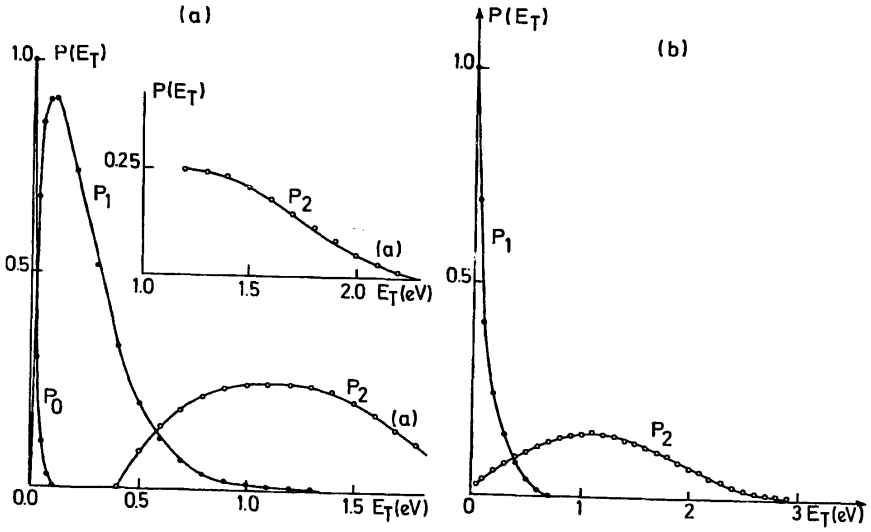

4. Discussion

The electron configuration of CH_3F in its ground electronic state could be described by the following outer valence-shell representation in the C_{3v} symmetry group:

$$(4a_1)^2(1e)^4(5a_i)^2(2e)^4.$$

By He(I) photoelectron spectroscopy the ionization energy of the X^2E, A^2A_1 and B ^2E states is measured [6]. Using the He(II) resonance line, the existence of a C $^2A_1$ state has been shown [7]. The photoelectron spectrum has been represented schematically in Fig. 2 and it shows that the X ^2E and the C $^2A_1$ states are isolated, contrarily the A^2A_1 and the B ^2E states are strongly interacting in the Franck-Condon region. Using photoelectron spectroscopic data [6,7], absorption spectroscopy in the vacuum UV [4] and appropriate thermochemical data [8], the correlation diagram in Fig. 5 has been built. In this diagram the Franck-Condon transitions are represented by shaded areas, the vertical rectangles locate the energy ranges where Rydberg states are observed in the absorption spectra of CH_3F. The R, R' and R" states converge to the X ^2E, B ^2E and C $^2A_1$ states respectively. With the help of these data the description of the dissociative ionization phenomena observed in

Published in: Chemical Physics (1996), vol. 206, pp. 225-236.
Status: Postprint (Author's version)

CH_3F could be attempted.

The X ^{2}E state of CH_3F has its adiabatic ionization energy at 12.533 eV [6] and the molecular ion is stable up to 13.35 eV. From PIPECO work [5], up from 13.35 eV the CH_2F^+ + H dissociation channel is open and these fragments appear at the expense of the X ^{2}E state only.

In the photoionization efficiency curve of CH_3^+ [4] two main processes are observed. The first appearance energy is measured at 14.55 eV in close agreement with the calculated threshold. Its cross section remains important at higher energies. The second threshold is observed at 16.25 eV, corresponding to an important increase of the cross section. This energy closely corresponds to the "adiabatic" ionization energy of the degenerate A^2A_1 + B ^{2}E states. Keeping in mind that the PIPECO results [5] show that the A^2A_1 + B ^{2}E states exclusively decay in the CH_3^+ + F channel, the lowest energetic process has unequivocally to be ascribed to an indirect dissociative ionization process involving the excitation of R'-type Rydberg states [4].

The 14.55 eV process is revealed by resonant photoionization [4] and from the present results obtained from Ne(I) excitation and gives rise to P_0 and P_1 translational energy distributions. The shape of both these distributions are believed to be ascribed to a quasi-statistical evolution of the X ^{2}E state indirectly populated by autoionization of the R' Rydberg states. This mechanism is still operative when Ne(I) radiation is used but concurrently with the direct population of the A^2A_1 + B ^{2}E over the narrow energy band ranging from 16.25 to 16.85 eV.

Fig. 5. *Correlation diagram for some dissociation channels in CH_3F^+. Shaded regions are Franck-Condon zones for direct ionization. Vertical rectangles locate the Rydberg series R, R' and R" converging to X ^{2}E, A^2A_1 and B ^{2}E states of CH_3F^+ respectively. The dashed curve tentatively locates the doubly excited electronic state decaying into CH_3^+ ($a^3A"$) + F.*

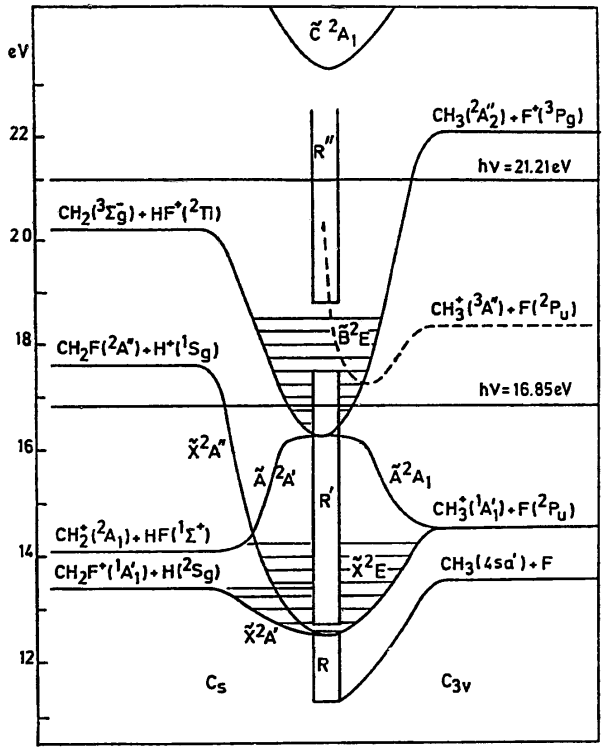

Confirming the PIPECO results [5], the second onset measured at 16.25 eV has to be ascribed to the excitation of the A^2A_1 + B ^{2}E states only. The shape of the corresponding TED curve is characteristic of the decay running over a strongly repulsive hyper-surface. In the Ne(I) excitation, the A^2A_1 state should be involved. Its decay looks strongly non-statistical, negatively surprised and submitted to many constraints. This appears from the occurrence of a nonzero threshold for E_T (0.4 eV) and from the strong curvature of the surprisal function (see Fig. 3a) [9].

Examining the results obtained with the He(I) radiation, it has to be pointed out that the P_2 distribution is also of the type observed for transitions taking place on a strongly repulsive surface, as it is the case with Ne(I) excitation. Small differences for 0.0 eV $\leq E_T \leq$ 3.0 eV have to be mentioned and are ascribed to the concurrent

Published in: Chemical Physics (1996), vol. 206, pp. 225-236.
Status: Postprint (Author's version)

population of the A^2A_1 state by a direct way and through a $B\ ^2E \rightarrow A^2A_1$ radiationless transition.

Concerning the P_2 distribution, it will be shown below (see Section 4.1.1) that it is also due to the sum of a zero translational energy component P_0 and of a quasi-statistical P, distribution differing strongly from the P_1 distribution observed with the Ne(I) lines ($0.0\ eV \leq E_T \leq 0.7\ eV$ instead of $0.0\ eV \leq E_T \leq 1.4\ eV$). It will be derived that P_1[Ne(I)] and P_1[He(I)] are statistical distributions expressed by $E_T^p \exp(-\beta E_T)$, but with significantly different values of the parameters p and β.

These subtle differences strongly suggest that the P_1[He(I)] distribution has to be assigned to an other dissociation channel $CH_3F^+ \rightarrow CH_3^+ + F$, i.e. through a population mechanism involving autoionization of R" Rydberg states (see Fig. 5). The CH_3F^+ electronic state involved, necessarily a doubly excited configuration of the molecular ion, will correlate with the CH_3^+ ($a^3A"$) + F dissociation limit at about 18.35 eV [11].

The role played by the autoionization of $R_1"$ and $R_2"$ Rydberg states is established by the appearance of small but well visible "bumps" in the CH_3^+ photoion yield curve in the energy range of the excitation of the Rydberg states converging to the CH_3F^+ ($C\ ^2A_1$) state. It has to be pointed out that these "bumps" are completely suppressed for a retarding potential of 0.45 V corresponding to a maximum E_T value of 0.8 eV, in excellent agreement with the measured P_1 distribution.

4.1. The detailed analysis of the P_1 distributions

4.*1.1. The P_1[Ne(I)] distribution*

The P_1[Ne(I)] distribution obtained in Fig. 4a has been deduced by the surprisal analysis of the total TED shown in Fig. lb (Ne). A mechanism has been proposed for its interpretation allowing us to give a better evaluation of the surprisal associated with this distribution.

This TED being entirely ascribed to the indirect population through autoionization of the CH_3F^+ ($X\ ^2E$) state, as autoionization is a resonant phenomenon, the $P^0(E_T/E_i)$ a priori statistical distribution expressed by Eq. (2) has to be evaluated for the unique value of $E = 2.3$ eV. The surprisal calculated on these bases is displayed in Fig. 6a. It appears positive and linear with a slope $\lambda = 2.66$. This implies that the P_1[Ne(I)] distribution is not rigorously statistical but not inverted. Klots [10] gave a theoretical expression which could reproduce the observed shape of the P_1[Ne(I)] distribution. It is based on the fact that the long range potential energy between the separating fragments is of the form $V = aR^{-n}$. When the long range potential is weakly attractive with a centrifugal potential, the $P(E_T)$ distribution is given by

$$P(E_T) = AE_T^p \exp(-\beta E_T), \qquad (7)$$

and when normalized to its maximum at E_M, it becomes

$$P(E_T) = \exp(p)\left(\frac{E_T}{E_M}\right)^p \exp\left(-\frac{\beta E_T}{E_M}\right). \qquad (8)$$

In this equation $p = n - 2/n$, where n is the exponent of R in the long range potential energy. It is worthwhile to note that Eq. (8) is closely related to Eq. (5). The reason is that when $E_T < E_i$ Eq. (2) can well be approximated as

$$P^0 \propto E_T^{0.5} \exp\left(-\frac{bE_T}{E_i}\right),$$

where $b = s + (r/2) - 1$.

As shown in Fig. 6b the best fit for P_1[Ne(I)] is given by

$$P_1(E_T) = 8.68\,E_T^{0.657} \exp(-6.48\,E_T). \qquad (9)$$

The shape of P_1[Ne(I)]being accounted for by Eq. (8) would imply that a restriction operates on the purely statistical behaviour of the $CH_3^+ + F$ decomposition. It should mainly be due to the balance between the long range potential between CH_3^+ and F and a centrifugal barrier. This explains the observed linear surprisal as ascribed to the occurrence of a unique constraint in the dynamics. The fact that the observed p value leads to $n \approx 6$, characteristic of a long range potential between neutral particles, instead of $n = 4$ for ion-neutral

Published in: Chemical Physics (1996), vol. 206, pp. 225-236.
Status: Postprint (Author's version)

interaction, does not be considered as very critical. As it appears from the work of Klots [10], the n value appears more as an adjustable parameter than as a stringent requirement. An example of this is given in the same paper where an agreement between theory and experiment is obtained only for $p = 1$ (or $n \rightarrow \infty$) in the case of the dissociation $C_6H_6^+ \rightarrow C_6H_5^+ + H$.

***Fig. 6**. (a) Surprisal associated with the indirectly populated P_1[Ne(I)] distribution and with respect to the distribution $P^0(E_T,E) = KE_T^{0.5}(2.3- E_T)^{6.5}$. The slope is $A_T = 2.66$. (b) Calculated P_1[Ne(I)] distribution by $P_1 = 8.68\, E_T^{0.657}\exp(-6.48\, E_T)$. (× × ×) Calculated, (o o o) experimental.*

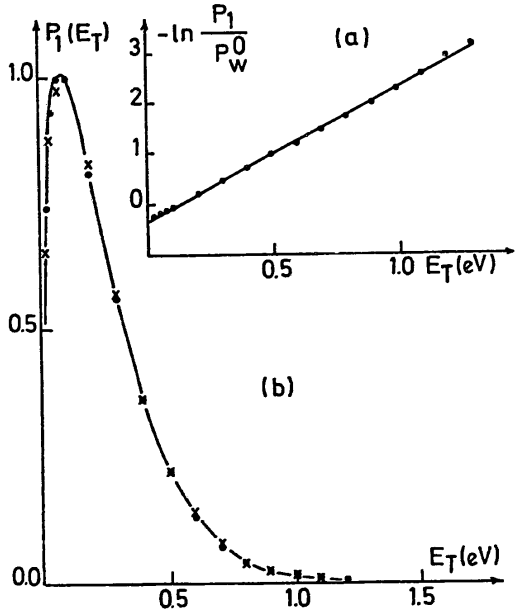

4.1.2. The P_1[He(I)] distribution

When the He(I) line is used the disentangling of the total TED shown in Fig. lb (He) leads to a P_1 distribution extending up to 0.7 eV with a maximum at $E_T = 0.0$ eV (see Fig. 4b). It has to be stressed that by 21.22 eV excitation the indirect population of two dissociation limits leading to CH_3^+ are possible, i.e. either the lowest limit at 14.55 eV

$$CH_3F^+ \rightarrow CH_3^+(X\,^1A_1') + F(^2P_u)$$

or the dissociation corresponding to

$$CH_3F^+ \rightarrow CH_3^+(a\,^3A'') + F(^2P_u)$$

calculated at 18.35 eV from the most recent theoretical calculations [11].

Considering that the excitation of a R" Rydberg level populates indirectly either the first or the second dissociation limit, two possible values of E have to be considered, i.e. 6.67 or 2.87 eV respectively. Consequently the surprisal of P_1[He(I)] was evaluated by using both these values introduced in Eq. (2).

As shown in Fig. 7a this operation leads to complex surprisals essentially linear above $E_T = 0.1$ eV. By a least-squares fit these linear parts are given by

$$-\ln\frac{P_1}{P^0(E_T/6.6)} = -0.039 + 6.533E_T, \qquad (10)$$

$$-\ln\frac{P_1}{P^0(E_T/2.85)} = 0.33 + 5.208E_T \qquad (11)$$

for $E_i = 6.67$ eV and $E_i = 2.87$ eV, respectively. By an extrapolation of both these straight lines for 0.0 eV $\leq E_T \leq$ 0.1 eV it is found that the P_1 distribution is a sum of a P_0 and a P_1' distribution (see Fig. 7a). The distribution

Published in: Chemical Physics (1996), vol. 206, pp. 225-236.
Status: Postprint (Author's version)

P_1' is accounted for by

$$P_1 = 6.46 E_T^{0.5} \exp(-7.602 E_T), \qquad (12)$$

corresponding to Eq. (7) where $p = 0.5$ or $n = 4$ corresponding to the exponent of a Langevin long range potential between CH_3^+ and F. The centrifugal potential plays an important role in the interaction between the two particles. The substantial differences between P_1[Ne(I)] and P_1'(He(I))] distributions have very likely to be ascribed to the correspondence of the latter distribution to the opening of the dissociation channel producing CH_3^+ (a^3A'')·

Fig. 7. *(a) Surprisals calculated for P_1[He(I)] for excess energies corresponding to two dissociation limits: E = 2.85 eV for $CH_3^+(^3A'')$ + F and E = 6.6 eV for $CH_3^+(^1A_1')$ +F. (b) Both surprisals led to the deconvolution of P_1 into P_0 and P_1'. (c) This latter distribution is fit by $P_0' = 6.46E_T^{0.5}\exp(-7.602E_T)$. (× × ×) Calculated, (o o o) experimental.*

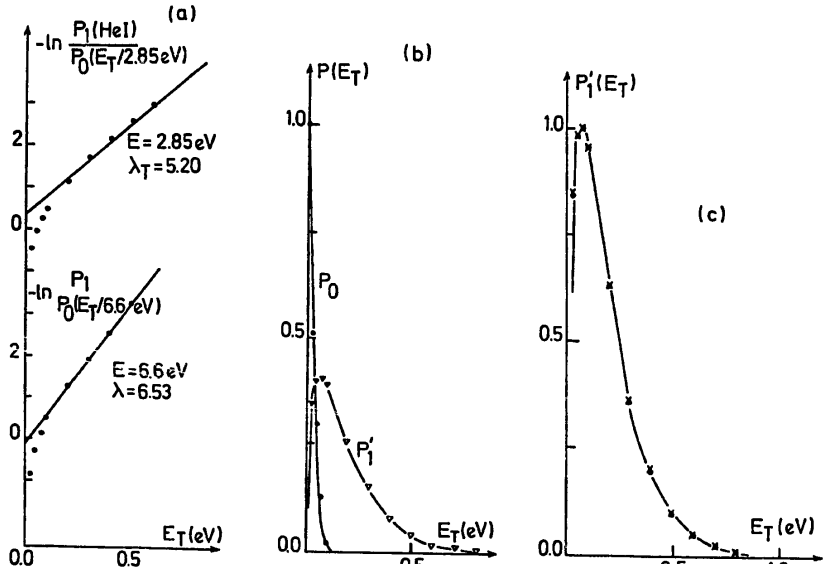

4.2. The detailed analysis of the P_2 distributions

4.2.1. The P_2[Ne(I)] distribution

As suggested earlier in this section, the P_2[Ne(I)] distribution has to be assigned to the direct population of a small part of the CH_3F^+ ($B\ ^2E$) state radiationlessly coupled with the A^2A_1 state where the dissociation takes place with a large amount total TED release. This distribution shows an important non-linear and negative surprisal (see Fig. 3a) which has to be expressed by a *n*th degree polynomial. It has been shown [9] that the degree *n* corresponds to the number of dynamical constraints of the dissociation. In an earlier work [12], the occurrence of a *4*th degree surprisal polynomial was assigned to four constraints. These constraints are introduced in the $P^0(E_T/E_i)$ expression to obtain a more accurate description of the P_2[Ne(I)] distribution.

A first limitation to be introduced in the function of $P^0(E_T/E_i)$ is that this function should be zero for E_T = 0.4 eV. To express this limitation in Eq. (2) one gets

$$P^0(E_T/E_i) = C_i(E_T - 0.4)^{0.5}(E_i - E_T)^{s+r/2-1}. \qquad (13)$$

This expression of P^0 introduced in the weighted function $\sum_i a_i P^0(E_T/E_i)$ will give a distribution P_w^0. The P_2 surprisal calculated with respect to this distribution is shown in Fig. 8. This surprisal is again non-linear and negative but with an initial slope of λ_T = - 4.92. This situation should correspond to the existence of severe limitations in the process and related to the number of vibrational degrees of freedom excited in CH_3^+.

Starting from the work of Busch and Wilson [13] related to the photofragmentation spectroscopy of

Published in: Chemical Physics (1996), vol. 206, pp. 225-236.
Status: Postprint (Author's version)

triatomic molecules, the H_3CF molecule could be considered as a triatomic $H_3{\equiv}C\text{-}F$ system. The dissociation of this molecule α-β-γ follows a pure impulsive model. In this framework, it has been shown that the E_T values are related to average excitation values E_{av} through the relationship

$$E_T = \frac{\mu_a}{\mu_f} E_{av}, \qquad (14)$$

where μ_a is the reduced mass of the two atoms α and β and μ_f is the reduced mass of α and $\beta\gamma$. In the present case taking E_{av} = 2 eV a value of E_T = 1.74 eV is determined and a rather restricted vibrational energy is left for CH_3^+, i.e. $E_{vibr.}$ = 0.26 eV. The most easily excited vibrational mode of CH_3 in CH_3I and CH_3Cl dissociations is the "umbrella" mode ω_2 [14]. In the CH_3F^+ dissociation only two quanta can be excited on the basis of Eq.(14) and choosing ω_2 = 0.17 eV, by analogy with infrared data on the isoelectronic BH_3 [15].

As it has been shown earlier [16], $P^0(E_T, E_v, E_i)$ has to be expressed by

$$P^0(E_T, E_v, E_i) = C_i(E_T - 0.4)^{0.5}(E_i - E_T - E_v)^{(r/2)-1} E_v^{s-1} \qquad (15)$$

and introducing in (15) the values s = 1 and r = 3, it becomes

$$P^0(E_T, E_v, E_i) = C_i(E_T - 0.4)^{0.5} \sum_{n=0}^{n} (E_i - E_T - n\omega_2)^{0.5}. \qquad (16)$$

As it appears from Section 3, the final P_w^0 is a weighted sum of $P^0(E_T, E_v, E_i)$ where the a_i factors are estimated from the A^2A_1 +B ^2E photoelectron band for each E_i value introduced in (16). This distribution is calculated in the 1.7 eV $\leq E_i \leq$ 2.3 eV range by steps of 0.1 eV and the summation is made for n = 0, 1 and 2 and is shown in Fig.8b. The rather good agreement between the experimental and calculated P_2[Ne(I)] distributions directly shows that the expression of the P_w^0 distribution evaluated through Eq. (16) and the severe constraints on the vibrational excitation of CH_3^+ in the direct dissociative ionization of CH_3F^+ are justified. This agreement is measured by the surprisal $-\ln(P_2/P_{theor})$ shown in the upper part of Fig. 8b. This surprisal is close to zero.

Fig. 8. *(a) Surprisal on P_2[Ne(I)] with respect to the distribution expressed by Eq. (13). (b) Experimental (o o o) and calculated (× × ×) P_2[Ne(I)] distribution using Eq. (16). The insert at the top of the diagram shows the residue.*

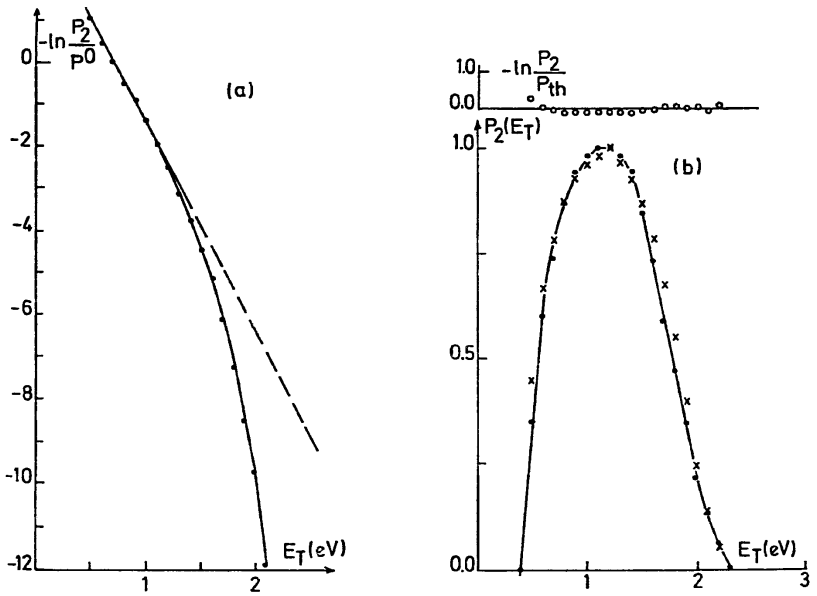

Published in: Chemical Physics (1996), vol. 206, pp. 225-236.
Status: Postprint (Author's version)

4.2.2. The P_2[He(I)] distribution

Using the surprisal calculated in Fig. 3b, the P_2 distribution shown in Fig. 4b looks different from the P_2[Ne(I)]. It starts at $E_T = 0$ eV and extends up to 3 eV, instead of 2.3 eV for Ne(I) excitation. The maximum is observed for $E_T = 1.1$ eV as for P_2[Ne(I)].

The linear and negative surprisal ($\lambda_T = -3.13$) shows that an inverted translational energy distribution is produced in this case. To build an a priori TED in agreement with P_2[He(I)] two hypotheses could be put forward: (i) a strong limitation on the number of excited vibrational levels in CH_3^+ and (ii) a non-$E_T^{0.5}$ dependence of the density of translational energy levels. On these bases a $P^0(E_T/E_i)$ has been calculated using $s = 1$ and the density of translational energy levels proportional to E_T

$$P^0(E_T/E_i) = C_i E_T (E_i - E_T)^{1.5}, \qquad (17)$$

and the P_w^0 distribution is estimated from

$$P_w^0 = \sum_i a_i E_T (E_i - E_T)^{1.5}. \qquad (18)$$

The E_i limits are 1.7 eV $\leq E_i \leq$ 4.0 eV scanned by 0.5 eV steps and the weighting factors a_i are measured from the $A^2A_1 + B\ ^2E$ photoelectron band.

Fig. 9 shows the comparison between calculation and experiment.

Table 1 *Relative abundance (%) of the total CH_3^+ ion yield for the P_0, P_1 (P_1') and P_2 distributions observed with the Ne(I) and He(I) resonance lines*

	P_0	P_1 (P_1')	P_2	$P_0/[P_0 + P_1 (P_1')]$
Ne(I)	3.6	51.2	45.2	6.6
He(I)	5.8	19.1	75.1	23.3

Fig. 9. *Experimental (o o o) and calculated (× × ×) P_2[He(I)] distribution using Eq. (18). The insert at the top of the diagram shows the residue.*

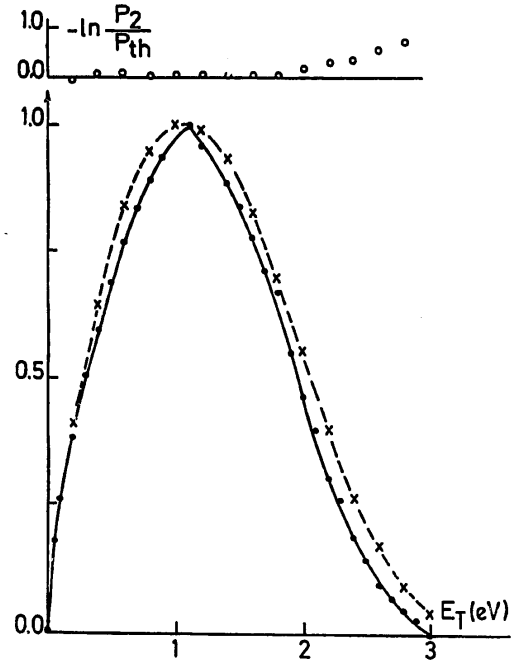

4.3. Relative importance of the distributions in the total CH_3^+ yield

Published in: Chemical Physics (1996), vol. 206, pp. 225-236.
Status: Postprint (Author's version)

The total surface of the distributions displayed in Fig. lb are practically equal, showing that the total CH_3^+ ion yield is almost constant for Ne(I) and He(I) excitation. This is also observed in the photoionization efficiency curve [4]. The fraction of this total abundance, spread over the P_0, P_1 (P_1') and P_2 distributions have been measured and are listed in Table 1.

This table shows that the distributions (P_0, P_1 and P_1') generated through indirect population by Ne(I) radiation are of about the same importance as those originating from the direct population (P_2). Contrarily, using He(I) as exciting radiation, the P_2 distribution becomes by far the most important contribution. It has also to be pointed out that the relative intensity of P_0 in $P_0 + P_1$ (P_1') is much more important when He(I) radiation is used.

4.4. Considerations about the P_0 distributions

As shown in Table 1 only a small part of the total CH_3^+ ion current contribute to the P_0 TED, for both the Ne(I) and He(I) excitation. The maximum is located at $E_T = 0.0$ eV and the distribution vanishes for $E_T \approx 0.1$ eV. In the frame of the RRKM theory for TEDs such distributions appear as entirely dominated by the characteristics of the transition state and their expression is given by [16]

$$P(E_T, E^*) = \left(1 - \frac{E_T}{E^*}\right)^{v-2}, \qquad (19)$$

where v is the number of vibrational degrees of freedom of the parent ion, i.e. $v = 9$ for CH_3F^+, and E^* is the excess energy above the zero point of the activated complex.

The P_0[Ne(I)] distribution is suitably expressed by Eq. (19) for an E^* value of 0.17 eV. Similarly, for the P_0[He(I)] distribution the E^* should be of 0.28 eV. On these bases it is possible to assign these P_0 distributions to a true RRKM-type decay of CH_3F^+ occurring at or very close to the dissociation limit. This behaviour is concurrent with the P_1 and the P_1' distributions where the angular momentum conservation should play an important role.

The differences observed between the P_0 distributions are accounted for by the two different "indirectly" populated dissociation limits, i.e. at (i) 14.55 eV with Ne(I) excitation and giving rise to

$$CH_3F^+(X\,^2E) \rightarrow CH_3^+(X\,^1A_1') + F(^2P_u)$$

and (ii) 18.35 eV with He(I) excitation and producing

$$CH_3F^+(a) \rightarrow CH_3^+(a\,^3A'') + F(^2P_u).$$

The CH_3F^+ (a) state is not observed in the He(I) photoelectron spectrum, being an electronic excited state of CH_3F^+ derived from a doubly excited configuration. However, its dissociation limit could be indirectly populated by autoionization of the R" Rydberg states converging to the CH_3F^+ ($C\,^2A_1$) state.

5. Conclusions

A careful surprisal analysis of the total TED observed for the appearance of CH_3 + F from CH_3F using 16.85 or 21.22 eV photons, coupled with the results obtained with other methods (photoionization, photoelectron spectroscopy, PIPECO spectroscopy) allowed us to show that at both energies direct and indirect population processes play an important role in dissociation dynamics.

Using the Ne(I) radiation, the indirect population of the CH_3F^+ ($X\,^2E$) state outside the Franck-Con-don region occurs through autoionization of Rydberg series converging to the $B\,^2E$ state. This process opens the possibility for the $X\,^2E$ state to dissociate at the thermodynamic limit by a "quasi"-RRKM mechanism. A narrow "RRKM" translational energy distribution P_0 appears concurrently with a positively surprised P_1 distribution. The surprisal is ascribed to strong angular momentum conservation.

Under the same conditions, the direct population of a limited portion of the CH_3F^+ ($B\,^2E$) state is followed by a non-radiative transition to the repulsive CH_3F^+ (A^2A_1) state correlated with the lowest dissociation limit. It gives rise to a non-linear negative surprisal for a P_2 distribution. This TED is shown to originate from a strongly limited excitation of the "umbrella" vibrational mode of CH_3^+ in the frame of the impulsive model for the energy partitioning.

Using the He(I) radiation, the indirect population of a doubly excited CH_3F^+ state takes place through autoionization of Rydberg series converging to the CH_3F^+ ($C\,^2A_1$) state. This state decays by a "quasi"-RRKM mechanism to the CH_3^+ (a^3A") + F dissociation limit at 18.35 eV. As for the first dissociation limit, a pure

RRKM TED P_0 is produced concurrently with a positively surprised P_1' distribution. The surprisal with respect to a pure statistical distribution is ascribed to strong angular momentum conservation.

Under these conditions the whole Franck-Condon region of the CH_3F^+ (B ^{2}E) state is reached. It is radiationlessly coupled with the strong repulsive A^2A_1 state. The dissociation process running over this path gives rise to a P_2 distribution characterized by a linear and negative surprisal. The strong negative surprisal is ascribed to (i) the excitation of a unique vibrational mode of CH_3^+ and (ii) the density of translational states proportional to E_T in the present case whereas it is proportional to $E_T^{0.5}$ in the framework of a statistical model.

Acknowledgements

We acknowledge the Université de Liège, the Fonds National de la Recherche Scientifique (FNRS) and the Fonds de la Recherche Fondamentale Collective (FRFC under contract No. 2.4532.95) for financial support.

References

[1] J. Momigny and R. Locht, Chem. Phys. Letters 211 (1993) 161.

[2] R. Locht, G. Caprace and J. Momigny, Chem. Phys. Letters 111 (1984) 560.

[3] J. Momigny, R. Locht and G. Caprace, Intern. J. Mass Spectrom. Ion Processes 71 (1986) 159.

[4] R. Locht, J. Momigny, E. Rühl and H. Baumgärtel, Chem. Phys. 117 (1987) 305.

[5] J.H.D. Eland, R. Frey, A. Kuestler, H. Schulte and B. Brehm, Intern. J. Mass Spectrom. Ion Phys. 22 (1976) 155.

[6] L. Karlsson, R. Jadrny, L. Mattsson, F.T. Chau and K. Siegbahn, Physica Scripta 16 (1977) 225.

[7] G. Bieri, L. Åsbrink and W. Von Niessen, J. Electron Spectry. Relat. Phenom. 23 (1981) 281.

[8] H.M. Rosenstock, K. Draxl, B.W. Steiner and J.T. Herron, J. Phys. Chem. Ref. Data Suppl. 1 6 (1977).

[9] A. Ben Shaul, Y. Haas, K.L. Kompa and R.D. Levine, Springer Series in Chemical Physics, Vol. 10. Lasers and chemical changes (Springer, Berlin, 1981).

[10] C.E. Klots, J. Chem. Phys. 64 (1976) 4269.

[11] J.A. Pople and P. von R. Schleyer, Chem. Phys. Letters 91 (1982) 9.

[12] J. Momigny, R. Locht and G. Caprace, Chem. Phys. 102 (1986) 275.

[13] G.E. Busch and K.R. Wilson, J. Chem. Phys. 56 (1972) 3626.

[14] H.W. Hermann and S.R. Leone, J. Chem. Phys. 76 (1982) 4766.

[15] J.R. Morrey, A.B. Johnson, Y.C. Fu and G.R. Hill, Advan. Chem. Ser. 32 (1961) 157.

[16] E. Illenberger and J. Momigny, Topics in Physical Chemistry, Vol. 2. Gaseous molecular ions (Steinkopff, Darmstadt; Springer, New York, 1992).